Practical Aspects of Aligning Asymmetric Top Molecules via Single-Photon Excitation: An Application to S 1 ← S 0 Excitation of Glyoxal

2 AUTHORS:

Miles Weida
Daylight Solutions Inc.
50 PUBLICATIONS **954** CITATIONS

SEE PROFILE

Charles S. Parmenter
Indiana University Bloomington
154 PUBLICATIONS **3,850** CITATIONS

SEE PROFILE

Practical Aspects of Aligning Asymmetric Top Molecules via Single-Photon Excitation: An Application to $S_1 \leftarrow S_0$ Excitation of Glyoxal

Miles J. Weida and Charles S. Parmenter*

Department of Chemistry, Indiana University, Bloomington, Indiana 47405

Received: August 5, 1997; In Final Form: October 2, 1997[⊗]

The practical aspects of aligning glyoxal (CHO−CHO) via $S_1 \leftarrow S_0$ photoexcitation with a linearly polarized laser are considered, with an emphasis on preparing the aligned molecules to probe for steric effects in crossed beam energy transfer. The degree to which "broadside" and "edge-on" collision geometries can be obtained for the planar glyoxal molecule is quantified. For a pump laser polarization parallel to the relative collision velocity, an aligned distribution is predicted in which a broadside collision is 2.3 times more likely than an edge-on collision. For the perpendicular laser polarization, an edge-on collision is 1.6 times more likely than a broadside collision. Implementation of alignment via photoexcitation in an actual experiment is described. Concerns when aligning molecules via this method are discussed, including saturation effects and nuclear spin depolarization. The laser-induced fluorescence formalism of Greene and Zare [*J. Chem. Phys.* **1983**, *78*, 6741] is used to demonstrate that glyoxal can indeed be aligned to the degree predicted by theory.

I. Introduction

Long before experimentalists were able to manipulate individual molecules to any significant extent, it was suggested that steric effects play an important role in chemical reactions and energy transfer. Based mostly on intuition, modifications of the Arrhenius equation to account for lower than predicted reactivities resulted in the inclusion of a steric factor.[1,2] The idea behind a steric factor is that only some of the many possible orientations between interacting molecules will result in a reaction or transfer of energy. The earliest demonstrations[3,4] of steric specificity in chemical reactions used a focusing electric hexapole field to orient the figure axis of methyl iodide before the reactive scattering event $CH_3I + M \rightarrow M + CH_3$, where M = K or Rb. An exceptionally high steric dependence was found, with reactions occurring predominately via collisions with the iodine end of the molecule. Since these classic experiments, a number of methods have been developed to control the relative collision geometries in scattering experiments (see ref 5 for an overview). Some of the most effective of these involve the use of lasers and intense optical fields to prepare molecules for probing steric effects. A necessarily incomplete list of these methods includes photoexcitation (reviewed in detail below) and selective depletion[6−8] with polarized lasers, stimulated Raman pumping,[9−11] laser-induced ac-Stark effects,[12] and interactions with intense, nonresonant laser fields.[13] Despite the number of demonstrated methods, the study of steric effects has remained a rather specialized endeavor, perhaps in part because the experimental techniques seem quite complex. We have found, however, that it is comparatively easy to obtain substantial control over the collision geometries of molecules in a crossed-beam experiment using the technique of photoexcitation with a linearly polarized laser. In the hopes of making such studies more accessible, we describe a practical application of this technique along with a discussion of the issues that need to be considered when preparing molecules for studying steric effects.

The photoexcitation method achieves a measure of spatial control over a molecular axis by *aligning* the molecule in the excited state. Alignment, and its companion orientation, are terms for describing the anisotropy in the spatial distribution of either the angular momentum vector **J** or a molecular axis. An aligned distribution has inversion symmetry, while an oriented distribution does not. In other words, it is possible to distinguish between the two ends of an oriented molecule, but only between the side and ends of an aligned molecule. Some intuition into how the photoexcitation method works can be gained by considering the semiclassical vibrational excitation of a diatomic molecule. If the internuclear axis is parallel to the polarization of the laser, the molecule is more likely to be excited than if the axis is perpendicular. Hence, the excited molecules end up with the internuclear axis directed predominately along the polarization vector. Although the quantum description is more complicated, this simple picture suggests how aligned excited-state molecules can be prepared via photoexcitation.

The initial theory for aligning linear and symmetric top molecules via photoexcitation was developed by Zare,[14] and several studies have exploited these results to search for steric effects in reactions. Pioneering experiments by Zare and co-workers include the reactive scattering of aligned $I_2^* + M \rightarrow MI^* + I$, where M = In or Tl,[15,16] and the reactive scattering of aligned $HF(v'=1) + Sr \rightarrow SrF + H$.[17,18] This technique was later employed by Loesch and co-workers[19] to observe steric effects in the reactive scattering of aligned $HF(v=1,j=2) + K \rightarrow KF + H$. HF is particularly amenable to studies of this type, since its reactivity increases by orders of magnitude upon vibrational excitation;[19] hence, infrared excitation can be used to both align HF and place it in a more reactive state. On the other hand, HF has nuclear spin that couples with the rotational motion to almost completely depolarize an aligned distribution for low-J states.[20] Therefore, Loesch and co-workers incorporate a Stark field in their experiment to decouple the nuclear spin from the overall rotation; HF optically excited in this field retains its initial alignment, enabling the study of reactive scattering for aligned $HF(v=1,j=1,m=0) + M \rightarrow MF + H$ for both M = Li[21,22] and Sr.[23,24] A summary of these experiments can be found in the review article by Loesch.[5] Finally, photoexcitation has also been used to probe for steric effects in vibrational energy transfer for low-energy collisions of excited $^1B_{2u}$ benzene in a supersonic expansion.[25] Although no steric

---

$S_1 \leftarrow S_0$ Excitation of Glyoxal

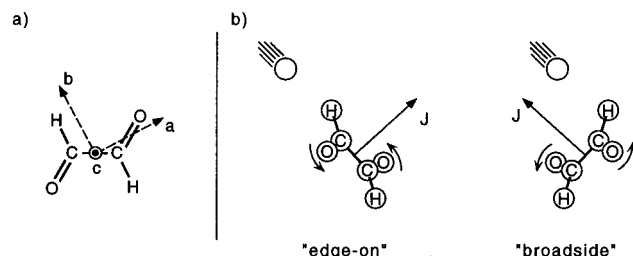*J. Phys. Chem. A, Vol. 101, No. 50, 1997* **9595**

Figure 1. (a) Schematic of *trans*-glyoxal with its principal axes. The *c* axis is perpendicular to the plane of the molecule. (b) Idealized collision geometries for testing for steric effects in collisional energy transfer with aligned glyoxal.

effects are observed, this study is novel for its use of photo-excitation to align a symmetric top.

Despite the demonstrated successes of aligning molecules via photoexcitation and the experimental simplicity of the method, it still remains relatively unused in scattering experiments. One reason might be that the initial theoretical treatment by Zare[14] only explicitly covers the alignment of linear and symmetric top molecules via parallel transitions. However, we have recently[26] extended Zare's theory to include perpendicular transitions and, more importantly, the whole class of asymmetric tops and their associated transitions. In these results, we find that the photoexcitation method is particularly powerful for aligning *all* of the axes of an asymmetric top. We would therefore like to explore the practicality of aligning asymmetric top molecules for crossed molecular beam study of inelastic scattering with controlled collision geometries.

The photoexcitation method can be conveniently applied to a series of crossed-beam experiments[27–30] in our laboratories probing translational to rovibrational energy transfer from S_1 glyoxal. Glyoxal (CHO−CHO), shown in Figure 1a, has many properties that make it amenable to such studies. First, it has several low-frequency in-plane and out-of-plane vibrations accessible at crossed-beam collision energies that can be monitored via fluorescence from the excited S_1 electronic state. Second, rotational states of glyoxal can be monitored via spectrally well-resolved rotational structure observable at moderate (1 cm^{-1}) resolution. Finally, the excited S_1 state has a ≈2 μs fluorescence lifetime, making it possible to pump glyoxal to a particular rovibrational state, where it then has time to experience a single collision before fluorescing. Rotational and vibrational states populated by inelastic processes can then be monitored via the dispersed fluorescence.

Glyoxal is an ideal candidate to prealign via the photoexcitation process by using a linearly polarized laser for the initial S_1 state preparation. However, there are many issues that first need to be considered. Ideally, the polarization of the excitation laser could be rotated such that "edge-on" or "broadside" collisions, shown schematically in Figure 1b, could be probed. Therefore, we need to determine how close we can come to these idealized collision geometries when using the photoexcitation technique, necessitating a theoretical treatment of aligning glyoxal. In addition to theory, there are issues of implementation. For example, the most effective experimental geometry for exploiting the photoexcitation technique needs to be determined, as well as the transitions that should be pumped to obtain maximum alignment. Finally, there are several practical aspects concerning the alignment of glyoxal that need to be considered. First, glyoxal has nuclear spin due to the H atoms; as demonstrated for HF,[20] this can depolarize the alignment for low-J states. Second, maximal alignment is attained via photoexcitation for unsaturated transitions. It would

be ideal to have a test to verify that molecules are being aligned and that effects such as depolarization or saturation are not a problem.

To address these issues for a practical application of aligning molecules via photoexcitation, the remainder of the paper covers the following. In section II the theoretically obtainable degree of alignment for glyoxal is determined, and the degree to which collision geometries are broadside or edge-on is quantified. Section III concerns the experimental implementation of the photoexcitation method. Special concerns associated with aligning molecules, as well as tests for verifying alignment, are covered in section IV. A summary is presented in section V.

II. Theory

The theory for aligning linear,[14,26] symmetric top,[14,26] and asymmetric top[26] molecules via photoexcitation has been worked out in detail, so we present a brief summary before considering the actual degree of alignment obtainable for glyoxal. Just as in the semiclassical description mentioned above, the photoexcitation method creates an aligned distribution of a molecular axis by exciting a subset of M levels. In the case of a P- or R-branch transition, photoexcitation with a linearly polarized laser results in **J** predominately perpendicular to the polarization of the light, much like one would expect for a semiclassical vibrational transition of a diatomic. For a Q-branch transition, however, the excited state **J** lies predominately *along* the polarization of the light. Hence, Q-branch transitions produce an opposite sense of alignment than P- or R-branch transitions.

The degree of alignment for each molecular axis can be determined by relating the excited-state distribution of rotational eigenstates to the spatial distribution of a molecular axis for a particular eigenstate. In general, this involves two parts. First the space-fixed projection of **J** following photoexcitation is determined, i.e., the M distribution. Second, the body-fixed projection of **J**, e.g., the K state for a symmetric top, is related to the space-fixed distribution of **J** to determine the actual space-fixed distribution of the molecular axis. If two conditions are met, i.e., (1) the initial distribution of M states is isotropic and (2) the transition is not saturated, then the molecular axis distribution resulting from photoexcitation with linearly polarized light can be expressed as

$$p(\theta) = [1 + \beta P_2(\cos \theta)]/4\pi \qquad (1)$$

where θ is the angle between the space-fixed polarization vector and the molecular axis of interest, $P_2(\cos \theta) = \frac{1}{2}(3 \cos^2 \theta - 1)$ is a second-order Legendre polynomial, and β is an anisotropy parameter[31] that describes the degree of alignment. The anisotropy parameter can range between -1 and $+2$, corresponding to a pure $\sin^2 \theta$ and $\cos^2 \theta$ distribution, respectively. For $\beta = +2$, the molecular axis is aligned along the polarization vector, while for $\beta = -1$, it is largely confined to a plane perpendicular to the polarization. Explicit equations for β for parallel and perpendicular transitions of linear and symmetric top molecules have been given,[14,26] and a prescription for determining β for each of the axes of an asymmetric top has been developed.[26] We have also made available a simple FORTRAN program[32] entitled ASYALIGN that determines the anisotropy parameter for each principal axis of an asymmetric top for a given transition.

Before considering glyoxal, we summarize the main results[26] concerning the alignment obtainable via the photoexcitation method. First, the degree of alignment depends only on J'', J', and the excited-state value of K for a symmetric top or K_a and K_c for an asymmetric top. It does *not* depend on the ground-
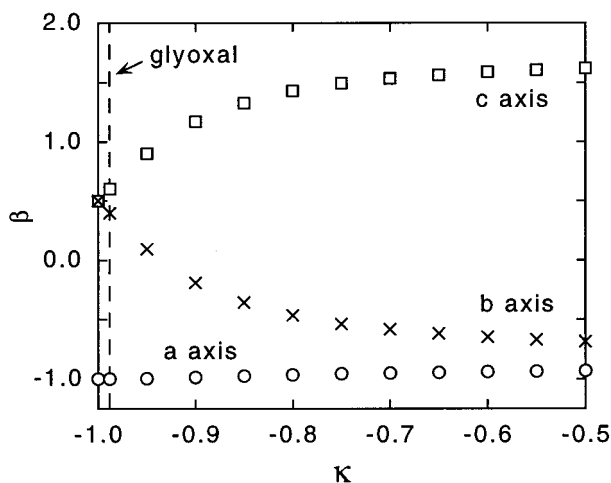
Figure 2. Anisotropy parameter β vs asymmetry parameter κ for 9_{09} $\leftarrow$ 9_{19} Q-branch excitation. This plot demonstrates the change in alignment for each of the principal axes as the asymmetry is increased from the prolate symmetric top limit. The alignment of the "figure axis," i.e., a inertial axis, is relatively unaffected by increasing asymmetry, while the b and c inertial axes actually become more aligned with increasing asymmetry. The effects of asymmetry on the degree of alignment for glyoxal ($\kappa = -0.988$) are negligible.

state value of K or K_a and K_c; hence, parallel or perpendicular type transitions can be used equally well to align symmetric and asymmetric tops. Second, Q-branch transitions tend to produce the highest degree of alignment, with an opposite sense than that for P- or R-branch transitions. Third, excited states where the projection of **J** on the figure axis of a symmetric top, or on the a or c axis of an asymmetric top, is at a maximum or minimum produce the maximum degree of alignment. Intermediate projections of **J** always produce less alignment. Finally, it is possible to highly align all three principal axes of a symmetric top when $K = J$, but only the figure axis when $K = 0$. However, asymmetric tops have a distinct advantage over symmetric tops in that a relatively small amount of asymmetry makes it possible to highly align all three principal axes even for states that correspond to $K = 0$ in the symmetric top limit.

We now turn to the issue of aligning glyoxal via photoexcitation. The planar glyoxal molecule (shown in Figure 1a) has rotational constants[33] for the 0° vibrational level of the excited S_1 state of $A = 1.964$ cm^{-1}, $B = 0.155$ cm^{-1}, and $C = 0.144$ cm^{-1}, making it an asymmetric top that is very close ($\kappa = -0.988$) to the prolate symmetric top limit. The $S_1 \leftarrow S_0$ transition moment is perpendicular to the plane of the molecule, so it is a c-type transition, or a perpendicular transition in the symmetric top limit. From theory,[26] the $K = 0 \leftarrow 1$ Q branch of a symmetric top is ideal for pumping to prepare an aligned distribution, since it has the unique property that the alignment of the figure axis is at a maximum, i.e., $\beta = -1$, and is *independent* of J state. Therefore, the analogous Q-branch for glyoxal is an ideal choice to prepare aligned states, since individual rotational transitions do not have to be resolved in order to prepare maximally aligned states.

Before we actually try to use this type of Q branch to prepare aligned states, it is necessary to determine the effects of asymmetry on the degree of alignment. Plotted in Figure 2 is the alignment of each of the principal axes of an asymmetric top for the $9_{09} \leftarrow 9_{19}$ transition as a function of increasing asymmetry from the prolate symmetric top limit. In asymmetric top notation, the transitions corresponding to the $K = 0 \leftarrow 1$ Q branch are either the b-type transitions $J_{0J} \leftarrow J_{1,J-1}$ or the c-type transitions $J_{0J} \leftarrow J_{1,J}$. (Remember, the ground-state values of K_a and K_c do not determine the degree of alignment.) In the
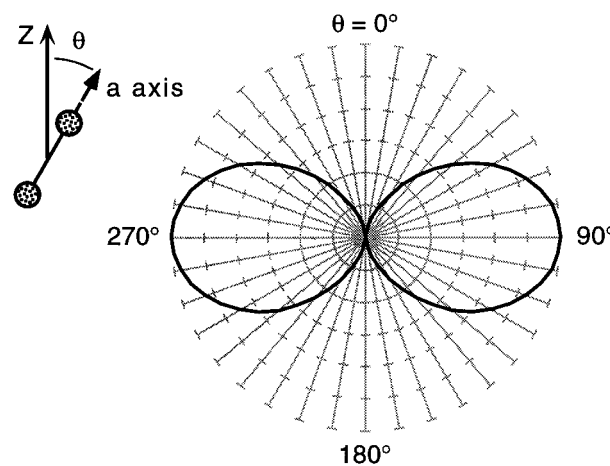

Figure 3. Polar plot of the distribution of the a axis for glyoxal after $K_a = 0 \leftarrow 1$ Q-branch absorption of light linearly polarized along the Z axis. The inset shows the relation between the a axis and the space-fixed Z axis.

prolate symmetric top limit, the alignment of the figure axis, i.e., the a axis, is at a maximum, as expected, and only decreases slightly as the asymmetry increases. The b and c axes, however, are relatively unaligned in the prolate limit. But as the asymmetry increases, the molecule begins to spin about the c axis, creating a high degree of alignment for all three axes. Glyoxal is close enough to the symmetric top limit that the effects of asymmetry are slight, and hence only the alignment of the a axis is extreme. As can be seen in the polar plot in Figure 3 for the axis distribution when $\beta = -1$, the a axis is almost completely confined to a plane perpendicular to the polarization vector.

We are interested, however, in the extent to which we can prepare broadside or edge-on collision geometries. Even if we know how the a axis is aligned, it does not provide enough information to determine whether a collision will correspond to these idealized geometries. The c axis, however, establishes how the plane of the molecule is aligned in space, since the c axis is perpendicular to this plane. If the relative collision velocity between glyoxal and some particle of interest lies along the c axis, then it will be a broadside collision. Likewise, if the c axis is perpendicular to the relative collision velocity, then it will be an edge-on collision.

To use the c axis to describe our idealized collision geometries, we follow Loesch and co-workers[19] in defining an angle of attack γ between the relative collision velocity $\mathbf{v}_{rel}$ and the c axis of glyoxal. The distribution of the c axis as a function of γ then provides a direct measure of the extent to which broadside ($\gamma = 0°$) or edge-on ($\gamma = 90°$) collision geometries can be prepared. If the polarization vector of the light lies along $\mathbf{v}_{rel}$, then $\gamma = \theta$, and the distribution in eq 1 can be used directly with the degree of alignment of the c axis in Figure 2 ($\beta = 0.603$ for the $9_{09} \leftarrow 9_{19}$ transition) to determine the distribution of the c axis as a function of angle of attack. As can be seen in Figure 4, for $\mathbf{v}_{rel}$ parallel to the polarization vector, glyoxal is 2.3 times more likely to suffer a broadside than an edge-on collision.

As might be expected, a distribution of collision geometries favoring edge-on collisions can be prepared by rotating the polarization of the light perpendicular to $\mathbf{v}_{rel}$. However, once this is done, $\gamma \neq \theta$, and we must reexpress eq 1 in terms of γ. The relation between θ and γ is given by[19]

$$\cos \theta = \cos \gamma \cos \alpha - \sin \gamma \cos \varphi \sin \alpha \qquad (2)$$

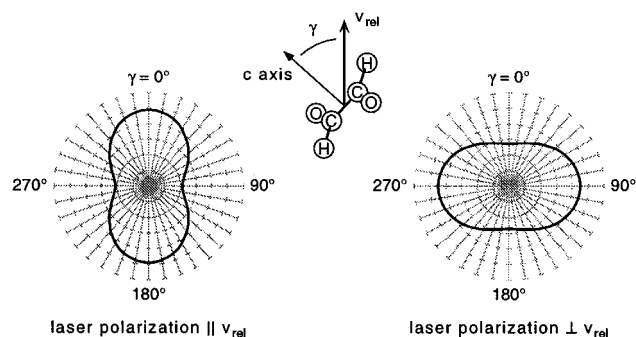where α is the angle between $\mathbf{v}_{rel}$ and the polarization vector,

S₁ ← S₀ Excitation of Glyoxal

J. Phys. Chem. A, Vol. 101, No. 50, 1997 **9597**

Figure 4. Angle of attack γ between the relative collision velocity $\mathbf{v}_{rel}$ and the c axis of glyoxal as a function of laser polarization angle for the $9_{09} \leftarrow 9_{19}$ transition of glyoxal. Since the c axis is perpendicular to the plane of glyoxal, collisions with $\mathbf{v}_{rel}$ parallel or perpendicular to the c axis are broadside or edge-on, respectively. With the laser polarization parallel to $\mathbf{v}_{rel}$, glyoxal is 2.3 times more likely to suffer a broadside than edge-on collision. With the polarization perpendicular to $\mathbf{v}_{rel}$, an edge-on collision is 1.6 times more likely than a broadside one.

and φ is an azimuthal angle about $\mathbf{v}_{rel}$. The presence of an azimuthal angle in eq 2 simply indicates that our distribution no longer has cylindrical symmetry with respect to $\mathbf{v}_{rel}$ when the polarization vector and $\mathbf{v}_{rel}$ are not parallel. In our instance, the polarization is rotated perpendicular to $\mathbf{v}_{rel}$, so $\alpha = 90°$, and the effective distribution of the c axis with respect to $\mathbf{v}_{rel}$ can be obtained by first substituting eq 2 in eq 1 and then integrating (i.e., averaging) over variations in φ. The resulting distribution is shown in Figure 4. As can be seen, the alignment of the c axis is not as great as when $\mathbf{v}_{rel}$ is parallel to the polarization vector, but nonetheless, we can prepare collisions this way such that an edge-on approach is 1.6 times more likely than a broadside approach.

It is worth mentioning that although glyoxal can be aligned via this method such that distributions favoring broadside or edge-on collision geometries are created, there are distinct advantages in using a molecule that has a slightly higher degree of asymmetry than glyoxal. Consider another test candidate for rovibrational energy transfer studies, D_2CO. It is still very nearly a prolate symmetric top, with $\kappa = -0.89$ in the ground state. However, the results in Figure 2 demonstrate that even this small degree of asymmetry is enough to cause D_2CO to spin predominately about the c axis when exciting the $K_a = 0 \leftarrow 1$ Q branch. Following the same arguments as above for the $9_{09} \leftarrow 9_{19}$ transition, we find that a distribution where a broadside collision is 4.6 times more likely than an edge-on collision can be prepared by rotating the polarization vector parallel to $\mathbf{v}_{rel}$ and a distribution where an edge-on collision is 2.8 times more likely than a broadside collision can be prepared for the polarization vector perpendicular to $\mathbf{v}_{rel}$. Hence, slightly more asymmetric tops provide a level of collision geometry control even greater than that obtainable for glyoxal.

III. Experimental Procedures

The theory results provide us with a method for probing for steric effects in vibrational and rotational excitation of glyoxal. By pumping the $K_a = 0 \leftarrow 1$ Q branch of glyoxal with linearly polarized light, and then rotating the polarization of the light such that it is either parallel or perpendicular to $\mathbf{v}_{rel}$, collision geometries that are predominately broadside or edge-on, respectively, can be prepared. We now consider the implementation of this method in an actual crossed-beam scattering experiment involving glyoxal.

Shown in Figure 5 is a schematic of the experimental apparatus. Approximately 5% glyoxal is seeded in He in the
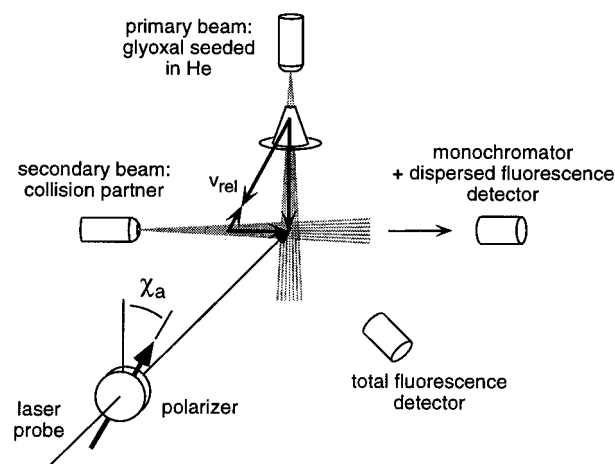

Figure 5. Experimental layout for aligning glyoxal in a crossed-beam experiment. The molecular beams and the pump laser are all mutually orthogonal. The linear polarization of the laser can be rotated either parallel or perpendicular to the relative collision velocity in order to create predominately broadside or edge-on collision geometries.

skimmed primary beam. At right angles to this is a secondary beam containing a collision partner of interest. The two beams intersect in the interaction region, where glyoxal is then pumped to a specific rovibrational state via S₁ ← S₀ electronic excitation with a pulsed dye laser ($\approx$10 ns pulse duration) at 455 nm. The beam densities are adjusted such that glyoxal has time to experience a single inelastic collision during its $\approx$2 μs fluorescence lifetime. States populated via inelastic processes are monitored via the dispersed fluorescence.

In previous experiments,[27-30] attempts were made to ensure that S₁ glyoxal was *un*aligned before the collisions. This was accomplished by using a nonorthogonal pump laser geometry and, more importantly, by saturating the transition of interest to destroy any anisotropy in the excited M state distribution. However, the results in section II demonstrate that it is a relatively simple matter to use the initial state preparation step to create our collision geometries of interest. To do this, a probe laser configuration is chosen that is mutually orthogonal to the two molecular beams. The linear polarization of the laser can then be rotated either parallel or perpendicular to $\mathbf{v}_{rel}$, since $\mathbf{v}_{rel}$ must always lie in the plane of the two beams. To establish the polarization angles to be used, it is necessary to first calculate the terminal velocity of each molecular beam based on established empirical formulas[34] and then perform a vector sum to determine $\mathbf{v}_{rel}$. Once this is done, the polarization can be rotated to prepare our broadside and edge-on collision geometries, taking care not to saturate the transition of interest. (Saturation effects will be discussed in section IV.)

At this point it is necessary to consider the preparation of the excited state by pumping the $K_a = 0 \leftarrow 1$ Q branch, on which our results in section II are based and for which we expect maximum alignment. Given a sufficiently narrow line width laser, it is no problem to pump individual rotational transitions in the jet-cooled glyoxal. However, we typically operate at moderate ($\approx$0.3 cm⁻¹) pump laser resolution, so there is a definite concern that the initial state preparation step will excite not just Q-branch transitions, but P- and R-branch transitions as well. Since these transitions result in an opposite sense of alignment than Q-branch transitions, this would significantly diminish our control over the collision geometries. However, consider the fluorescence excitation spectrum in Figure 6a for the 0_0^0 band of glyoxal at a pump laser resolution of 0.3 cm⁻¹. The band is structured, with pronounced features corresponding to either Q-branches or P- or R-branch band heads for each K_a'
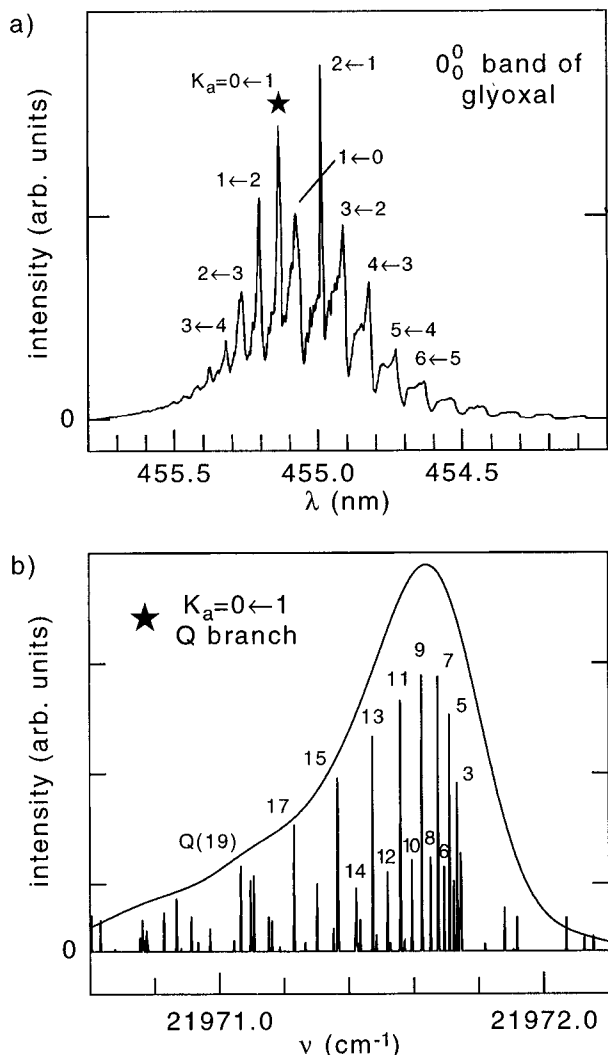
a)

b)

Figure 6. (a) Fluorescence excitation spectrum for the 0_0^0 band of the $S_1 \leftarrow S_0$ transition of *trans*-glyoxal (from ref 27). At a resolution of 0.3 cm^{-1}, many sharp features occur that correspond to either Q branches or band heads (conditions: 5% glyoxal in He, 0.5 mm skimmed pinhole nozzle, $T_{rot} \approx 30$ K). (b) Predicted spectrum for the $K_a = 0 \leftarrow 1$ Q-branch region at resolutions of 0.3 and 1.8 × 10^{-3} cm^{-1}. As can be seen, the sharp spectral feature marked by a star in a) is comprised almost entirely of $K_a = 0 \leftarrow 1$ Q-branch transitions. (The predicted spectra are based on the spectroscopic constants[33] of glyoxal with $T_{rot} = 30$ K. The alternating intensity pattern is due to nuclear spin statistics.)

$\leftarrow K_a''$ transition. With the help of predicted spectra based on the fitted rotational constants[33] of glyoxal and a predicted rotational temperature of 30 K, it is possible to zoom in on the feature associated with $K_a = 0 \leftarrow 1$, labeled with a star in Figure 6a. As can be seen in Figure 6b, this feature consists almost entirely of Q-branch transitions, providing an ideal spectral region to pump with only moderate (0.3 cm^{-1}) laser resolution to access just the Q branch.

As mentioned previously, the degree of alignment is at a maximum and *independent* of J for the $K = 0 \leftarrow 1$ Q branch of a symmetric top. Since glyoxal is so close to the symmetric top limit, each of the final states will have nearly the same degree of alignment when pumping the feature marked with a star in Figure 6, even though a distribution of J states will be excited (typically from $J = 3$ to 11 at our resolution). This uniformity greatly simplifies the analysis and enables us to prepare the broadside and edge-on collision geometry distributions shown in Figure 4 simply by rotating the linear polarization of the pump laser.

IV. Discussion and Results

Although we have predicted the maximum degree of alignment attainable for glyoxal and the experimental geometry best suited for preparing broadside and edge-on collision geometries, there are several effects that can decrease the alignment from the theoretical maximum. Perhaps the most serious of these is depolarization from nuclear spin or external fields. In addition, the predicted degree of alignment is predicated upon the initial distribution of M levels being isotropic and the pump transition being unsaturated; deviations from these requirements can also adversely affect the alignment obtainable via photoexcitation. We therefore discuss these issues and then consider several tests that can be used to verify the degree of alignment. Finally, the laser-induced fluorescence (LIF) formalism of Green and Zare[35] is implemented to establish that glyoxal can be aligned to the extent predicted by theory.

A. Factors Affecting Alignment. *1. Depolarization.* One of the first molecules aligned via photoexcitation, i.e., HF, turned out to be problematic because of the presence of nuclear spin in the molecule. Although HF was initially considered to be an ideal candidate for aligning by vibrational excitation with the R(0) transition, subsequent studies[18,20] revealed that the alignment created for the $J = 1$ level is "depolarized" by the presence of nuclear spin in HF. Hence, more recent studies[5] employ a Stark field to decouple the nuclear spin from the rotation. Depolarization turns out to be a general effect for molecules with nuclear spin and has been treated theoretically[20,36] and observed in detail experimentally[37,38] for aligned HF and HCl. Since glyoxal has nuclear spin on each of the H atoms, depolarization is a potential concern and must be addressed.

The semiclassical description of nuclear spin depolarization is relatively uncomplicated. The nuclear spin **I** does not interact strongly with the angular momentum **J** (including all forms of angular momentum except nuclear spin) and hence can be viewed as being uncoupled from the internuclear framework of the molecule. When a molecule undergoes photoexcitation, the orientation of **J** is affected, but **I** remains randomly distributed in the space-fixed frame. After photoexcitation, **J** is aligned but immediately begins to precess around the total angular momentum vector **J** + **I**. This precession decreases the initial degree of alignment, especially when **J** and **I** are of the same magnitude.

The quantum description[20,36] of nuclear spin depolarization is actually more instructive than the semiclassical description. Nuclear spin angular momentum is technically no different than the other forms of angular momentum that constitute **J**, i.e., nuclear rotation, electron spin, and electronic orbital angular momentum. Therefore, one could use the total angular momentum **F** = **J** + **I** when working out the theoretical aspects of aligning a molecule via photoexcitation. However, the coupling between **J** and **I** is generally weak enough that transitions from levels with different **F** but the same **J** are not resolved in most experiments. When these transitions are pumped to create aligned molecules, multiple **F** states are excited, necessitating a description of the alignment that includes a coherent excitation of states with different angular momenta. This leads to a quantum beat phenomenon, such that the alignment of the excited state varies with time in a recurring fashion. For HF, these oscillations are generally on the order of a few microseconds;[20,38] hence, for most experiments the net alignment is best described by a depolarization coefficient averaged over the temporal variations. It must be stressed that this type of depolarization is not due to nuclear spin per se, but to the unresolved hyperfine structure. For example, if splittings

S$_1$ ← S$_0$ Excitation of Glyoxal

J. Phys. Chem. A, Vol. 101, No. 50, 1997 **9599**

due to electron spin were not resolved, the same effect would be observed and might be called electron spin depolarization.

As mentioned above, nuclear spin depolarization is most pronounced when **J** and **I** are of the same magnitude and becomes rapidly less important for $J > I$. In their study of HF, Altkorn et al.[20] show that a nuclear spin of $^1/_2$ on both the H and F atoms is sufficient to almost totally depolarize the alignment of **J** for $J = 1$ but that the depolarization effect becomes relatively negligible for $J > 3$. Since glyoxal has nuclear spin comparable to HF, the depolarization should be insignificant when exciting $J > 3$. However, in the absence of measured hyperfine coupling constants to actually predict the depolarization, it is necessary to have a test to determine that depolarization is not decreasing the initial alignment.

In addition to depolarization due to unresolved hyperfine structure, external magnetic[39] and electric[40] fields can also affect the degree of alignment after the initial photoexcitation step. The depolarization due to magnetic fields is known as the Hanle effect,[39] and for molecules with significant magnetic dipole moments even the magnetic field of the earth can affect the alignment of **J**. Although the stray fields present in our laboratory are not anticipated to be strong enough to cause significant depolarization of **J** for glyoxal, some test is needed to verify that this is actually the case.

2. Saturation. One of the assumptions behind the alignment theory is that the initial pump transition is not saturated. Practically, this requires that an experiment be operated in a linear regime to obtain the degree of alignment predicted by theory. For direct absorption or LIF, either the absorbance or the fluorescence intensity, respectively, must scale linearly with incident laser power. If the excitation occurs in a nonlinear regime, then the relative population difference between M levels begins to decrease from that expected for the linear regime. Since a high degree of alignment depends on a large degree of anisotropy in the M distribution, the lessening of the anisotropy through saturation only serves to decrease the degree of alignment. Although there have been several treatments[41−43] of alignment in a nonlinear regime, these in general are more complicated than the alignment theory we have dealt with so far and also require that the degree of saturation be quantified. Therefore, it is beneficial both for the degree of alignment and the simplicity of the theory to operate in a linear regime.

Operating in a linear regime is a fairly exacting requirement, which ultimately limits the number of molecules that can be aligned in the excited state. For example, the total fluorescence intensity of glyoxal after S$_1$ ← S$_0$ excitation of the 0$_0^0$ band with a pulsed dye laser ($\approx$10 ns pulse duration) as a function of incident pulse energy is shown in Figure 7. Deviations from nonlinearity are obvious for incident energies as low as 10 μJ/pulse. The measurements in Figure 7 are performed with the laser beam size expanded to $\approx$0.25 cm^2 via a Galilean telescope in order to more evenly distribute the laser power and push the linear regime to higher incident pulse energies. However, nonlinearity still sets in at fairly low energies. To push the laser power to the limit of the linear regime and thus create more aligned molecules in the excited state, a test is necessary to verify that saturation effects are not diminishing the degree of alignment.

3. Prealignment of Molecules. The last issue that needs to be addressed is any prealignment of glyoxal that occurs in the supersonic expansion before photoexcitation. The second key assumption of the theory in section II is that the initial M distribution is isotropic. However, it has been shown in several experiments[44−47] that linear molecules seeded in a lighter carrier gas are moderately aligned in a supersonic expansion. Although
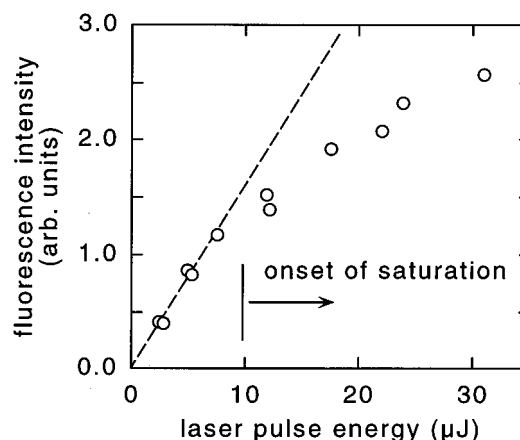
Figure 7. Total fluorescence intensity of the 0$_0^0$ band of glyoxal vs incident S$_1$ ← S$_0$ pump laser energy. Note that deviations from linearity occur for energies as low as 10 μJ/pulse. Conditions: pulsed dye laser with $\approx$10 ns pulse duration at 455 nm, pumping $K_a = 0$ ← 1 Q branch.

this degree of alignment is relatively small compared to the alignment that can be achieved by photoexcitation, it does have the potential to affect the degree of alignment obtainable via photoexcitation. Therefore, a test is needed to verify that the glyoxal is not being significantly prealigned in the supersonic expansion.

B. Tests for Verifying Alignment. When all of these concerns are taken into account, two separate tests are needed to verify that glyoxal is being aligned. The first test is to verify that the initial M distribution is isotropic. Obviously, if the molecule to be aligned is in a static cell with a thermal distribution, no tests are necessary to verify that the M distribution is isotropic. As noted above, however, supersonic expansions can align molecules, so we therefore list some of the tests to establish that the initial M distribution is isotropic. (1) Perhaps the most general method to measure alignment is via direct absorption coupled with polarization modulation.[46] Changes in measured absorbance with changes in polarization of the light can be related to the alignment of the molecules being probed. (2) If the molecules are amenable to probing via LIF, the formalism of Greene and Zare[35] can be used to measure the alignment by relating changes in fluorescence intensity to changes in the polarization of the pump laser and the detected fluorescence. This technique has been extended to saturated conditions as well.[43] A variant of the LIF method involves using a magnetic field to rotate **J** and then determining the degree of alignment from changes in fluorescence intensity with changing magnetic field.[48] (3) If the molecule is paramagnetic, then individual M levels can be resolved using magnetic field gradients.[47] Alternately, the M distribution can be measured for molecules amenable to focusing via hexapole fields.[49−51] (4) Finally, alignment can be detected via optical pumping methods[52] and two-photon absorption.[53] Although not a complete list, this gives an idea of the many possible techniques available to test for alignment.

The second test is needed to determine whether the final excited state is aligned to the degree that theory predicts and thus whether depolarization or saturation effects are important. Although any of the tests mentioned above can also be used to probe the alignment of the final state, most have the disadvantage that a second laser or additional apparatus is necessary in addition to the laser used to create the alignment. The one exception to this is the LIF technique coupled with an LIF pump/probe experiment, since the laser used to create the aligned state can also be used to determine the alignment of the initial state, and the polarization of the fluorescence can be used to measure
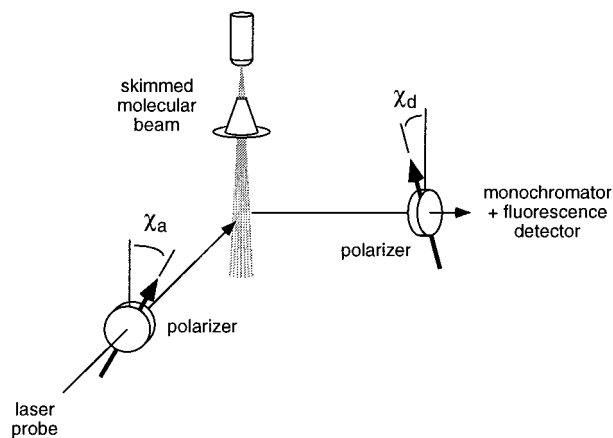
Figure 8. Mutually orthogonal probe/detection geometry for verifying alignment. The polarization angles, χ_a and χ_d, are with respect to the molecular beam axis.

Figure 9. Monochromator response as a function of dispersed fluorescence polarization angle χ_d. The blaze pattern of the diffraction grating leads to markedly different transmission efficiencies depending on whether the light is polarized parallel or perpendicular to the ruled lines on the grating. Here, $\chi_d = 33°$ corresponds to light polarized parallel to the grating lines. The fitted curve is a $\cos^2$ distribution.

the alignment of the excited state. In addition, the LIF technique has already been shown to be an effective means for determining the alignment created by photoexcitation. For example, the polarization of the fluorescence following two-photon excitation of NO has been used[54] to establish the laser-induced alignment of the excited state. Since the glyoxal experiment employs LIF, we describe this technique in more detail and present results of our tests on aligning glyoxal via photoexcitation.

C. LIF Tests for Glyoxal. The use of LIF to detect alignment is based on some of the same ideas used in section II to describe the alignment process via photoexcitation. Basically, unsaturated excitation via a polarized pump laser creates an anisotropic distribution of M. If $\mathbf{J}$ is not depolarized during the time it takes for the molecule to fluoresce, then the anisotropy in M leads to some degree of polarization of the fluorescence. Greene and Zare[35] have worked out the degree of fluorescence polarization expected for the excitation/detection geometry shown in Figure 8. The experimental geometry shown in Figure 5 can be modified accordingly by inserting a polarization analyzer before the dispersed fluorescence collection. The intensity of the fluorescence will then depend on (1) the polarization of the pump laser, i.e., χ_a, (2) the polarization of the detected fluorescence, i.e., χ_d, (3) the transition being pumped and the transition being monitored, and (4) any initial alignment of the molecules.

To use Greene and Zare's results, it is necessary to pump a particular transition, and then monitor a particular transition. As shown in Figure 6, it is relatively simple to pump just $K_a = 0 \leftarrow 1$ Q-branch transitions of glyoxal. However, the fluorescence from these excited states occurs in the form of P-, Q-, and R-branch transitions. Therefore, it is necessary to disperse the detected fluorescence to monitor just Q-branch transitions. To determine the feasibility of restricting our fluorescence detection to just Q-branch transitions, we calculated the $S_0 \leftarrow S_1$ dispersed fluorescence spectrum for glyoxal based on the fitted rotational constants,[33] a pump laser resolution of 0.3 cm^{-1}, and an initial rotational distribution at 30 K. We find that if the maximum of the dispersed fluorescence $K_a = 1 \leftarrow 0$ Q branch is monitored at a monochromator resolution of 1 cm^{-1}, there is only an 8% contribution to the total intensity from P- and R-branch transitions. Hence, it is possible to restrict the observed fluorescence almost entirely to Q-branch transitions. However, given our current experimental arrangement, we do not have sufficient resolution to monitor individual transitions within this highly overlapped Q branch.

Although the theory for detecting alignment is relatively straightforward given the excitation and detection polarizations
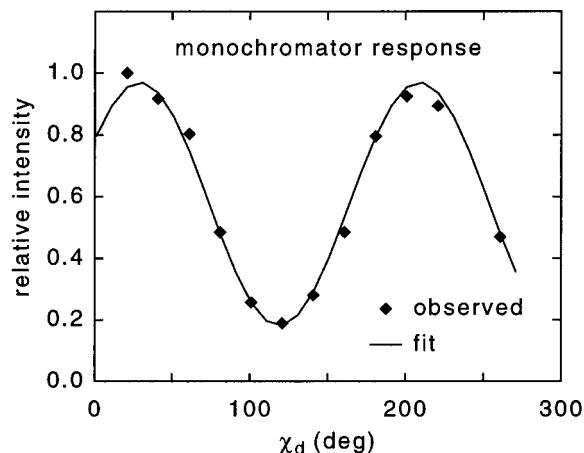
plus the transitions being excited and detected, the presence of a dispersive element, in this case a 1.7 m Czerny-Turner monochromator, complicates the analysis by introducing a high degree of birefringence into the fluorescence detection path. The birefringence is due chiefly to the blaze of the diffraction grating,[55] which in our case leads to a relative transmission efficiency for light polarized perpendicular to the grating lines that is a factor of 5 smaller than for light polarized parallel to the grating lines. Clearly, a polarization response function for the monochromator plus detection optics is needed before the alignment can be measured.

To determine such a response function requires an unpolarized light source. Various unpolarized sources were tried, but the overall polarization response function is highly sensitive to the exact position the unpolarized light is emitted from with respect to the collection optics. Therefore, we used an in situ calibration in the form of unpolarized light from the excitation and detection of glyoxal itself in the molecular beam. According to the formalism of Greene and Zare, the intensity of the fluorescence should be independent of χ_d for the detection geometry in Figure 8 with $\chi_a = 90°$, provided that the initial sample of glyoxal is unaligned. Of course, this is what we are trying to determine, so this method of calibration is somewhat circular. However, we would not expect the alignment of glyoxal seeded in He to be significantly greater than that for CO_2 seeded in He. Using the measured[46] upper limits for the alignment of CO_2 in He with the formalism of Greene and Zare, we predict that the peak-to-peak fluctuation in fluorescence intensity as a function of χ_d for $\chi_a = 90°$ should be less than 9%. This small fluctuation still provides more certainty in determining the polarization response function as compared to the problems associated with trying to place another unpolarized light source into the correct location of our detection optics. The resulting response function is shown in Figure 9; the variations in transmitted intensity with polarization are well represented by a $\cos^2(\chi_d)$ distribution.

Once we have determined the polarization response function, it is possible to measure the true degree of polarization of the fluorescence for $\chi_a = 0°$. This geometry is expected to provide the maximum polarization of the fluorescence. The uncorrected intensities are recorded as a function of χ_d and then normalized using the response function in Figure 9. As can be seen in Figure 10, the resulting variations in fluorescence intensity as a function of χ_d are as great as 60% when exciting and detecting a Q-branch transition. The predicted variation in intensity based
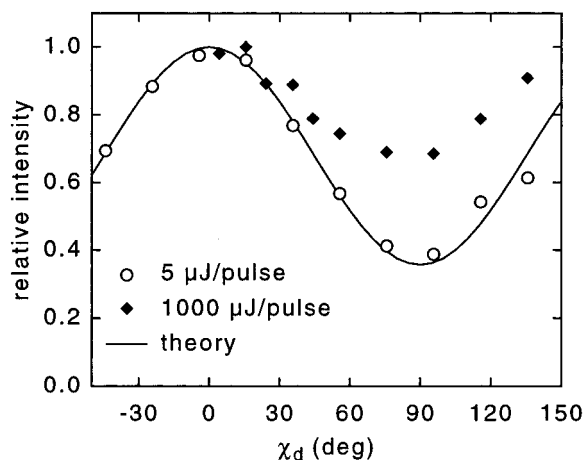
Figure 10. Relative fluorescence intensity as a function of detection polarization angle χ_d. This is for a mutually orthogonal detection geometry with $\chi_a = 0°$, an arrangement that should produce the maximum polarization of the fluorescence. Theory[35] is for pumping and observing the Q(3) transition. Notice how saturating the transition degrades the degree of alignment.

on the LIF theory of Green in Zare[35] for an unaligned initial sample is also shown in Figure 10. The results in Figure 10 are for pumping and detecting on the Q(3) transition, in correspondence with the $J = 3-11$ distribution of states that are pumped. We note that the variation in fluorescence intensity is 6% greater for Q(11) and attribute the small difference between the observed variation and that predicted for the higher J states in the distribution to the 8% contamination of P- and R-branch transitions in the dispersed fluorescence. As can be seen, however, the measured degree of polarization is in agreement with theory for an unaligned initial distribution of **J**, and no depolarization of **J** before glyoxal fluoresces.

The results in Figure 10 tell us several things. First, the agreement with theory for an unaligned initial distribution is strong evidence that the glyoxal is not significantly prealigned by the supersonic expansion. Even though it was assumed that the glyoxal is initially unaligned when determining the polarization response function of the monochromator and detection optics, significant prealignment would still show up as deviations from theory in Figure 10. Second, these results indicate that glyoxal is not being significantly depolarized by either nuclear spin or external fields during its fluorescence lifetime. Since the theory of Greene and Zare requires the preparation of the same M distribution as in the photoexcitation experiment in order for the predicted degree of fluorescence polarization to be observed, the agreement between theory and experiment provides direct confirmation that the glyoxal is being aligned as indicated and that depolarization is not a problem. Independent measurements[56] in our laboratories of glyoxal fluorescence intensities as a function of excitation and detection polarizations for various transitions are also in agreement with theory, providing additional confirmation that depolarization is not a problem for glyoxal aligned via photoexcitation.

Last, tests under nonlinear conditions in Figure 10 demonstrate how the alignment created by photoexcitation can be severely degraded when saturating the transition. The two different powers shown in Figure 10 correspond to a regime where the fluorescence intensity has a linear dependence on the laser pump power, i.e., 5 μJ/pulse, and a highly nonlinear regime, i.e., 1 mJ/pulse. As can be seen, the decrease in fluorescence polarization is consistent with a less aligned distribution of **J** in the excited state. This test provides a clear indication of the maximum laser powers that can be employed to align glyoxal via photoexcitation. As long as the laser powers

are kept within a linear regime, there should be no problem in obtaining the theoretically predicted degree of alignment.

V. Summary

A practical application of the photoexcitation method for aligning glyoxal via S₁ ← S₀ excitation demonstrates that it is relatively simple to prepare highly aligned molecules for probing steric effects in crossed-beam experiments. In addition, such an application provides an opportunity to highlight some of the practical concerns when aligning molecules, as well as diagnostics for determining whether molecules are truly being aligned via the photoexcitation method. In particular, effects such as nuclear spin depolarization, depolarization due to external fields, prealignment of the molecules via supersonic expansions, and saturation need to be considered. Of the several possible tests to verify alignment, a particularly easy one to implement for experiments employing laser excitation with fluorescence detection involves measuring the fluorescence intensity as a function of laser excitation and fluorescence detection polarizations. This method enables one to test for prealignment of the molecules and whether depolarization or saturation effects are important. The results indicate that glyoxal is indeed highly aligned via photoexcitation, such that the theoretically predicted edge-on or broadside collision geometries can be prepared simply by rotating the linear polarization of the laser either perpendicular or parallel to the relative collision velocity.

References and Notes

(1) See, for example: Hinshelwood, C. N.; Winkler, C. A. *J. Chem. Soc.* **1936**, 371.
(2) See, for example: Adam, N. K. *Physical Chemistry*; Oxford: London, 1954.
(3) Brooks, P. R.; Jones, E. M. *J. Chem. Phys.* **1966**, *45*, 3449.
(4) Beuhler, J., Robert J.; Bernstein, R. B.; Kramer, K. H. *J. Am. Chem. Soc.* **1966**, *88*, 5331.
(5) Loesch, H. J. *Annu. Rev. Phys. Chem.* **1995**, *46*, 555.
(6) Dehmelt, H. G.; Jefferts, K. B. *Phys. Rev.* **1962**, *125*, 1318.
(7) De Vries, M. S.; Sradnov, V. I.; Hanrahan, C. P.; Martin, R. M. *J. Chem. Phys.* **1983**, *78*, 5582.
(8) Drullinger, R. E.; Zare, R. N. *J. Chem. Phys.* **1969**, *51*, 5532.
(9) Band, Y. B.; Julienne, P. S. *J. Chem. Phys.* **1992**, *96*, 3339.
(10) Dopheide, R.; Zacharias, H. *J. Chem. Phys.* **1993**, *99*, 4864.
(11) Sitz, G. O.; Farrow, R. L. *J. Chem. Phys.* **1994**, *101*, 4682.
(12) Linskens, A. F.; Dam, N.; Reuss, J.; Sartakov, B. *J. Chem. Phys.* **1994**, *101*, 9384.
(13) Friedrich, B.; Hersbach, D. R. *Chem. Phys. Lett.* **1996**, *262*, 41.
(14) Zare, R. N. *Ber. Bunsen-Ges. Phys. Chem.* **1982**, *86*, 422. Note that the denominator in eq 18 should read $J''(2J'' + 1)$.
(15) Estler, R. C.; Zare, R. N. *J. Am. Chem. Soc.* **1978**, *100*, 1323.
(16) Rettner, C. T.; Wöste, L.; Zare, R. N. *Chem. Phys.* **1981**, *58*, 371.
(17) Karny, Z.; Estler, R. C.; Zare, R. N. *J. Chem. Phys.* **1978**, *69*, 5199.
(18) Zhang, R.; Rakestraw, D. J.; McKendrick, K. G.; Zare, R. N. *J. Chem. Phys.* **1988**, *89*, 6283.
(19) Hoffmeister, M.; Schleysing, R.; Loesch, H. *J. Phys. Chem.* **1987**, *91*, 5441.
(20) Altkorn, R.; Zare, R. N.; Greene, C. H. *Mol. Phys.* **1985**, *55*, 1.
(21) Loesch, H. J.; Stenzel, E.; Wüstenbecker, B. *J. Chem. Phys.* **1991**, *95*, 3841.
(22) Loesch, H. J.; Stienkemeier, F. *J. Chem. Phys.* **1993**, *98*, 9570.
(23) Loesch, H. J.; Stienkemeier, F. *J. Chem. Phys.* **1994**, *100*, 740.
(24) Loesch, H. J.; Stienkemeier, F. *J. Chem. Phys.* **1994**, *100*, 4308.
(25) Whetton, N. T. Ph.D. Thesis, Flinders University of South Australia, 1991.
(26) Weida, M. J.; Parmenter, C. S. *J. Chem. Phys.* **1997**, *107*, 7138.
(27) Butz, K. W.; Du, H.; Krajnovich, D. J.; Parmenter, C. S. *J. Chem. Phys.* **1988**, *89*, 4680.
(28) Gilbert, B. D.; Parmenter, C. S.; Krajnovich, D. J. *J. Phys. Chem.* **1994**, *98*, 7116.

(29) Gilbert, B. D.; Parmenter, C. S.; Krajnovich, D. J. *J. Chem. Phys.* **1994**, *101*, 7423.

(30) Gilbert, B. D.; Parmenter, C. S.; Krajnovich, D. J. *J. Chem. Phys.* **1994**, *101*, 7440.

(31) We have chosen to identify β as an anisotropy parameter instead of an alignment parameter in order to avoid confusion with the more commonly used alignment and orientation parameters $A_0^{(2)}$ and $O_0^{(1)}$, which describe the anisotropy in the *M* distribution. Since the molecular figure axis is perpendicular to **J** for $K = 0$, β and $A_0^{(2)}$ can have different signs and values for the same *M* distribution, creating confusion if both are called an alignment parameter.

(32) Weida, M. J.; Parmenter, C. S. ASYALIGN computer code; distributed by Quantum Chemistry Program Exchange: Vol. 17, program no. 675, Indiana University, 1997.

(33) Birss, F. W.; Brown, J. M.; Cole, A. R. H.; Lofthus, A.; Krishnamachari, S. L. N. G.; Osborne, G. A.; Paldus, J.; Ramsey, D. A.; Watmann, L. *Can. J. Phys.* **1970**, *48*, 1230.

(34) Scoles, G. *Atomic and Molecular Beam Methods*; Oxford University Press: New York, 1988.

(35) Greene, C. H.; Zare, R. N. *J. Chem. Phys.* **1983**, *78*, 6741.

(36) Greene, C. H.; Zare, R. N. *Annu. Rev. Phys. Chem.* **1982**, *33*, 119.

(37) Orr-Ewing, A. J.; Simpson, W. R.; Rakitzis, T. P.; Zare, R. N. *Isr. J. Chem.* **1994**, *34*, 95.

(38) Zhang, J.; Riehn, C. W.; Dulligan, M.; Wittig, C. *J. Chem. Phys.* **1996**, *104*, 7027.

(39) Zare, R. N. *Acc. Chem. Res* **1971**, *4*, 361.

(40) Zare, R. N. *J. Chem. Phys.* **1966**, *45*, 4510.

(41) Altkorn, R.; Zare, R. N. *Annu. Rev. Phys. Chem.* **1984**, *35*, 265.

(42) Janssen, M. H. M.; Parker, D. H.; Stolte, S. *Chem. Phys.* **1987**, *113*, 357.

(43) Meyer, H.; Leone, S. R. *J. Chem. Phys.* **1996**, *105*, 5858.

(44) Sinha, M. P.; Caldwell, C. D.; Zare, R. N. *J. Chem. Phys.* **1974**, *61*, 491.

(45) Pullman, D. P.; Friedrich, B.; Herschbach, D. R. *J. Chem. Phys.* **1990**, *93*, 3224.

(46) Weida, M. J.; Nesbitt, D. J. *J. Chem. Phys.* **1994**, *100*, 6372.

(47) Aquilanti, V.; Ascenzi, D.; Cappelletti, D.; Pirani, F. *J. Phys. Chem.* **1995**, *99*, 13620.

(48) Visser, A. G.; Bekooy, J. P.; van der Meij, L. K.; de Vreugd, C.; Korving, J. *Chem. Phys.* **1976**, *20*, 391.

(49) Brooks, P. R. *Science* **1976**, *193*, 11.

(50) Parker, D. H.; Bernstein, R. B. *Annu. Rev. Phys. Chem.* **1989**, *40*, 561.

(51) Bulthius, J.; van Leuken, J. J.; Stolte, S. *J. Chem. Soc., Faraday Trans.* **1995**, *91*, 205.

(52) Hefter, U.; Ziegler, G.; Mattheus, A.; Fischer, A.; Bergmann, K. *J. Chem. Phys.* **1986**, *85*, 286.

(53) Meyer, H. *Chem. Phys. Lett.* **1994**, *230*, 510.

(54) Kessler, W. J.; Poliakoff, E. D. *J. Chem. Phys.* **1986**, *84*, 3647.

(55) Stroke, G. W. *Phys. Lett.* **1963**, *5*, 45.

(56) Loge, G. W.; Parmenter, C. S. *J. Chem. Phys.* **1981**, *74*, 29.